

Review Article

A plane-based approach for the characterization of supraspinatus tendon tear at the footprint in MRI

Anuradha Sharma¹, Kirti Gehlot¹, Sagar Tomar², Mahesh Kumar¹, Nishith Kumar¹, Dharmendra Kumar Singh¹

¹Department of Radiodiagnosis, VMMC and Safdarjung Hospital, New Delhi, ²Department of Radiodiagnosis, Neo Hospital, Noida, Noida, Uttar Pradesh, India.



***Corresponding author:**
Dharmendra Kumar Singh,
Department of Radiodiagnosis,
VMMC and Safdarjung
Hospital, New Delhi, India.

dksinghrad@gmail.com

Received: 23 November 2021
Accepted: 15 February 2022
Epub Ahead of Print: 15 April 2022
Published: 23 June 2022

DOI
10.25259/IJMSR_54_2021

Quick Response Code:



ABSTRACT

Rotator cuff tears are a common cause of persistent shoulder pain and the supraspinatus tendon (SST) is the common culprit. The zonal demarcation of the tendon with advances in MR imaging has identified the SST footprint to be the common location of tear within the SST. Identification and characterization of such tears are important as such tears are a treatable cause of shoulder pain, thereby preventing long-term shoulder instability. This article intends to present a plane-based approach for the characterization of footprint tears of SST on MRI which will help in reporting by the practicing radiologists and radiology residents.

Keywords: Supraspinatus tendon tear, Supraspinatus footprint tear, Rim-rent tear, Delamination tear, Longitudinal tear

INTRODUCTION

Among the four tendons which constitute the rotator cuff (RC), the supraspinatus tendon (SST) is the most frequently injured. This is on account of the synergistic effects of extrinsic acromial impingement and intrinsic tendon degeneration. Previously, the critical zone was considered the common site of SST tears. However, it has now been demonstrated that tear at the footprint is the common location of SST tears.^[1] Various classifications of SST tear at footprint have been proposed over the years.^[2-5] The purpose of the article is to present a novel plane-based approach for describing SST tears at the footprint.

ANATOMY

The RC of the shoulder comprises four muscles and their tendons: Subscapularis (SSC), SST, infraspinatus (IST), and teres minor (TM). The RC unit acts as a dynamic stabilizer of the glenohumeral joint.^[6] The previous viewpoint was that the four tendons of the RC had separate insertions onto the humeral tubercles, leading to discrete individual tendon footprints. SSC, which inserts onto the lesser tubercle, was thought to have an auricular footprint. SST, IST, and TM insert onto the superior, middle, and inferior aspect of the greater tubercle, respectively; with corresponding separate triangular or trapezoidal impressions on the greater tubercle “[Figure 1].”^[7,8] However, studies have shown the RC tendon fibers interdigitate with one another, and their deepest layer also fuses with the joint capsule before their common insertion onto the humeral footprints. An interdigitation between SSC and SST is present at the bicipital groove, creating a pulley over the long head of the biceps tendon. Another site of interdigitation is

This is an open-access article distributed under the terms of the Creative Commons Attribution-Non Commercial-Share Alike 4.0 License, which allows others to remix, transform, and build upon the work non-commercially, as long as the author is credited and the new creations are licensed under the identical terms.

©2022 Published by Scientific Scholar on behalf of Indian Journal of Musculoskeletal Radiology

present between SST and IST around 15 mm proximal to their common insertion onto the greater tubercle.^[9,10]

Anatomically, the SST has been divided into anterior, middle, and posterior thirds. The anterior third of the SST attaches to the anterior half of the superior facet of the greater tuberosity, the middle third of the SST attaches to the posterior half of the superior facet of the greater tuberosity, and the posterior third of the SST interlinked with IST tendon attaches to the superior half of the middle facet of the greater tuberosity “[Figure 2].”^[3] An important point to note is that the attachment of the SST extends from the articular margin medially to the superior facet of the greater tuberosity laterally “[Figure 3].”^[7] Hence, even deepening of the sulcus evidenced by extension of joint fluid or intra-articular gadolinium-based contrast agent into the space between the humeral articular margin and greater tuberosity is an indicator of partial-thickness articular-sided tears of the SST.

The SST is formed by five layers. From bursal to articular surfaces, the layer 1: Fibers of coracohumeral ligament, layer 2: Densely packed fibers in parallel orientation, layer 3: Randomly oriented smaller fibers, layer 4: Loose connective tissue, and layer 5: Articular capsule [Figure 4], with an average thickness of the tendon ranging between 9 and 12 mm.^[11]

Histologically, like most other tendons, tenocytes are the most populous cell type within the SST as well, which are responsible for the production of extracellular matrix. Less abundant cell types are myocytes, synoviocytes, and endothelial cells; later in blood vessels.^[12] Based on the extracellular matrix composition, the insertion of the SST



Figure 1: Volume rendering technique image of upper humerus demonstrates footprints of rotator cuff tendons. The areas marked in green, red, blue, and yellow represent the footprint of the subscapularis, supraspinatus, infraspinatus, and teres minor tendons, respectively. The bicipital groove is demonstrated by a red asterisk.

is divided into four zones from medial to lateral. There is a gradual transition rather than a sharp demarcation between these zones. The first zone is tendinous, predominantly comprising type I collagen with small amounts of proteoglycan decorin. The second zone is fibrocartilaginous and mostly has collagen types II and III, with small amounts of proteoglycans. The penultimate zone is mineralized fibrocartilage made of collagen types II and X, as well as the proteoglycan aggrecan. The last zone is osseous, composed of type I collagen with high mineral content. With tendon degeneration, the tenocytes tend to become rounder in shape with increased apoptosis; and the extracellular matrix becomes less organized with fatty degeneration.^[13]

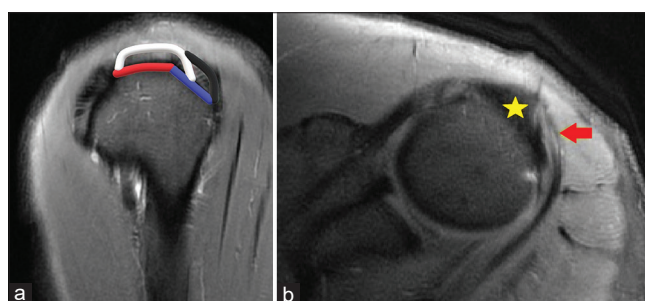


Figure 2: Oblique sagittal (a) and axial (b) proton-density fat saturation MR images of the shoulder joint. “(a)” Attachment of supraspinatus tendon (area represented by a white line) to the superior facet (red line) of the greater tuberosity. The posterior fibers of the supraspinatus tendon are interlinked with the infraspinatus tendon (area represented by a black line) and are attached to the superior half of the middle facet (blue line) of the greater tuberosity. “(b)” Overlapping of posterior fibers of supraspinatus (yellow asterisk) with infraspinatus tendon (red arrow) at the middle facet of the greater tuberosity.

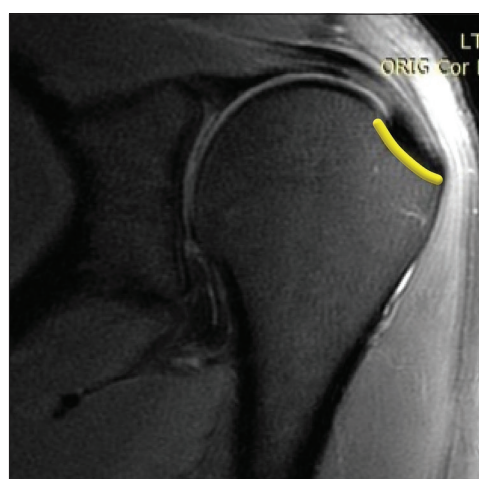


Figure 3: Oblique coronal proton-density fat saturation MR image of shoulder joint demonstrates footprint of the supraspinatus tendon (yellow line) that extends from the articular margin medially to the superior facet of the greater tuberosity laterally.

SUPRASPINATUS TEAR

Tendon injuries/tendinopathy of the RC is among the most common problems of the shoulder, affecting not only sports persons but also those performing repetitive activities related to work or daily living as well.^[14-16] Moreover, RC tendinopathies increase with age; affecting more than 80% of people over 80 years of age.^[16,17] These tears can cause pain and varying degrees of movement restriction and can disrupt daily living. SST is inherently prone to tear and subacromial impingement has the synergistic effect in this regard. Hence, the SST has the maximum tendency to tendinopathy/tears and is the most commonly affected of the RC tendons.^[18-20] Apart from tears due to tendon degeneration and repetitive microtrauma, SST tears may also occur as a result of an acute traumatic event such as a fall on the outstretched hand. In these circumstances, the tears occur because the stresses within the RC exceed the tensile strength of the tendon.^[21]

Tears of the RC tendons can be classified as partial-thickness or full-thickness tears. Further, partial-thickness tears can be subclassified based on location as either bursal sided or articular sided. Lesions involving the mid-substance of the tendon are called interstitial tears.^[22,23]

Most SST tears, especially degenerative ones, occur in a relatively hypovascular region approximately 1 cm medial to the tendon insertion. This is called “critical zone” “[Figure 5].”^[24] However, as far back in 1934, Codman had described a situation in which SST fibers were “torn-out” of the bony insertion at the greater tubercle, which he named as “rim-rent tears.”^[25] Subsequently, Vinson *et al.* concluded that rim-rent tears involving the insertional fibers of the RC were the most common type of partial-thickness RC tear. Moreover, on imaging, many



Figure 4: A schematic diagram of the supraspinatus tendon demonstrates layers of tendon composition (layers 1–5).

full-thickness RC tears appeared as if they originated as rim-rent tears and progressed afterward to involve the full thickness of the tendon.^[1] Understanding the biomechanical importance of the RC footprint is one of the anatomical basis for the surgical repair of RC tears. Active and earlier intervention enables the patient to return to a pre-injury level, hence, timely and accurate assessment of the RC footprint tear on magnetic resonance (MR) imaging is required.^[26,27]

Ellman proposed the following arthroscopic classification for partial-thickness RC tears at the footprint, which was later extrapolated to imaging as well [Figure 6].^[2]

Grade I: Partial-thickness tear involving 1–2 mm of the tendon insertion at the greater tuberosity.

Grade II: Partial-thickness tendon tear with a vertical defect involving $\leq 50\%$ thickness (3–6 mm) of the footprint.

Grade III: Partial-thickness tendon tear and an extension $>50\%$ thickness (>6 mm) of the tendon insertion at the greater tuberosity.

However, this classification only takes into account the vertical extension of the tear. The horizontal component (delamination) and longitudinal components of tear have not been taken into consideration.

Schaeffeler *et al.* classified the RC footprint tears into four types [Figure 7].^[3]

1. Partial-thickness articular surface supraspinatus tendon avulsion (PASTA) lesions: If there is a discontinuity and retraction of articular tendon fibers.
2. Concealed interstitial delamination (CID): If there is an interstitial tear in the tendon, not extend to the articular/bursal surface.



Figure 5: Oblique coronal proton-density fat saturation MR image of shoulder joint demonstrates partial thickness tear in the “Critical Zone” of the supraspinatus tendon (red arrow).

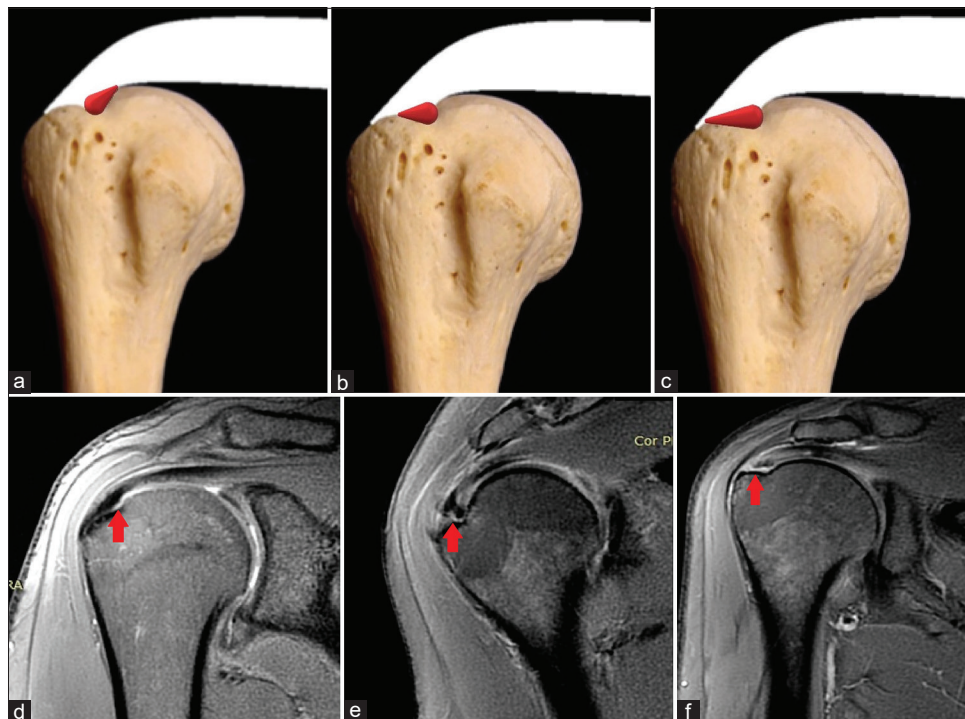


Figure 6: Schematic diagrams of the supraspinatus tendon (a-c) and representative oblique coronal proton-density fat saturation MR images (d-f) of the shoulder joint. The red areas in schematic diagrams and red arrows in representative MR images demonstrate Ellman's classification of partial-thickness tear at the footprint of supraspinatus tendon: Grade I in “(a and d);” Grade II in “(b and e);” and Grade III in “(c and f).”

3. Bursal-sided tendon avulsion (reverse PASTA) lesions: If there is a discontinuity and retraction of bursal tendon fibers.
4. Full thickness tear: If there is a full-thickness tendon tear from bursal to the articular surface along with retraction. This classification also has certain drawbacks. It has not taken into consideration the geometry of the tear (U- or L-shaped longitudinal split tear). Furthermore, it has not detailed the delamination tears other than the CID. Both of these are important determinants of the type of arthroscopic repair procedure to be undertaken.

Delamination refers to intratendinous horizontal splitting between the articular and bursal layers of the SST with or without different degrees of retraction between the two layers.^[5,28] Dissimilar stress between two layers of the RC has been postulated as cause of delaminated tears. The delamination tear has been classified into six types [Figure 8].^[5]

- i. Type 1a: Articular-delaminated full-thickness tear defined as a full-thickness tear in which the articular layer is more medially retracted than the bursal layer, with or without an intratendinous horizontal splitting tear.
- ii. Type 1b: Bursal-delaminated full-thickness tear defined as a full-thickness tear in which the bursal layer is more medially retracted than the articular layer, with or without an intratendinous horizontal splitting tear.

- iii. Type 1c: Intratendinous-delaminated full-thickness tear defined as a full-thickness tear in which the articular layer is equally retracted to the bursal layer, combined with an intratendinous horizontal splitting tear.
- iv. Type 2a: Articular delaminated partial-thickness tear defined as an articular surface partial-thickness tear with an intratendinous horizontal splitting tear.
- v. Type 2b: Bursal-delaminated partial-thickness tear defined as a bursal surface partial-thickness tear with an intratendinous horizontal splitting tear
- vi. Type 2c: Intratendinous-delaminated partial-thickness tear defined as an isolated intratendinous horizontal splitting tear (CID).

Various surgical procedures are performed for the repair of supraspinatus footprint tears. Delamination tears are managed by procedures such as interlaminar curettage, layer-to-layer suturing, flap resection, and additional suture fixation across the delaminated area. On the other hand, longitudinal tears are typically mobile in an anteroposterior direction and can usually be repaired by a side-to-side/margin convergence technique.^[29-31] The management of rim-vent tears is controversial. Some surgeons operate only on full thickness tears. Other surgeons have a different school of thought that laterally located rim-vent tears can also cause pain so they perform arthroscopic debridement of such partial tears as well.^[26,32]

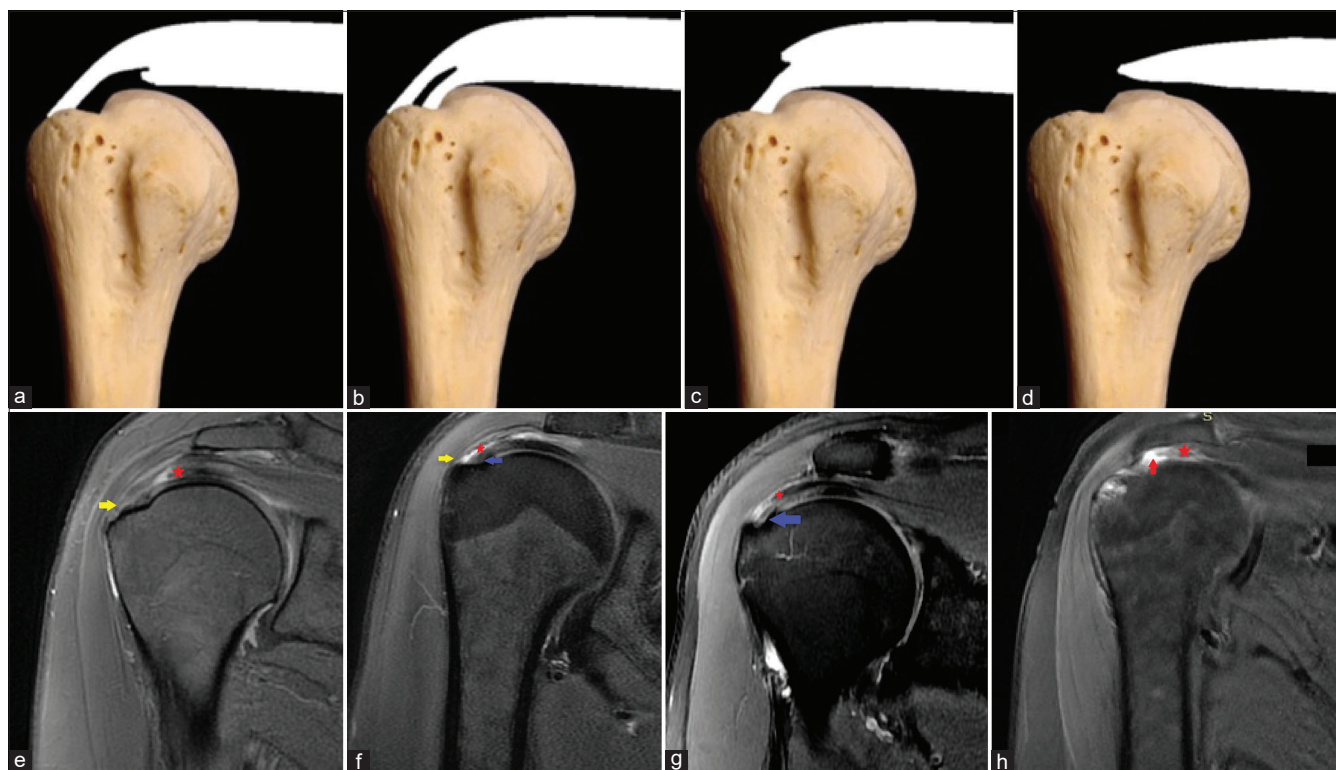


Figure 7: Schematic diagrams of the supraspinatus tendon (a-d) and representative oblique coronal proton-density fat saturation MR images (e-h) of shoulder joint demonstrate a defect in supraspinatus tendon articular surface in “(a)” and representative partial articular-sided supraspinatus tendon avulsion (PASTA) from footprint (red asterisk: Retracted articular fibers and yellow arrow: Attached bursal fibers) in “(e).” Interstitial defect in supraspinatus tendon is demonstrated in “(b)” and representative interstitial delamination tear (red asterisk) splitting between articular fibers (blue arrow) and bursal fibers (yellow arrow) is demonstrated in “(f).” Defect in the bursal surface of the supraspinatus tendon is demonstrated in “(c)” and representative partial bursal-sided supraspinatus tendon avulsion (reverse PASTA) from the footprint (red asterisk: Retracted bursal fibers and blue arrow: Attached articular fibers) in “(g).” Full-thickness defect in supraspinatus tendon is demonstrated in “(d)” and representative full-thickness tear with retraction (red asterisk) is demonstrated in “(h).” In full-thickness tear, the joint cavity communicates with subacromial-subdeltoid bursa (red arrow).

MR ACQUISITION FOR THE SHOULDER JOINT

MR imaging of the shoulder joint is performed using a surface coil (dedicated shoulder coil) with the patient in a supine position with the arm at the side in a neutral position or slight external rotation. A small field of view (12–14 cm) and 3–4 mm thick slices are obtained in three orthogonal planes: Coronal oblique plane (parallel to SST/in a plane perpendicular to the articular surface of glenoid), sagittal oblique plane (parallel to the articular surface of glenoid), and axial plane (from top of the acromion to bottom of glenohumeral joint). MR sequences for the evaluation of RC injury include proton-density fat-suppressed sequences (coronal oblique, sagittal oblique, and axial) as well as T2-weighted coronal oblique, gradient echo coronal oblique, and T1-weighted sagittal oblique sequences.^[33]

Shoulder MR arthrography is required in the evaluation of shoulder instability and is routinely done in suspected

RC tears. The MR arthrography is extremely useful for delineation of partial-thickness articular surface SST tear. The cocktail used for shoulder arthrogram consists of 0.1 ml of gadolinium mixed with 20 ml of normal saline, 3 ml of iodinated contrast. About 12–13 ml of the mixture is injected into the shoulder joint under fluoroscopic guidance before MR acquisition. For ultrasound-guided injection, iodinated contrast is not required in the cocktail. The MR sequences for shoulder arthrogram include T1 fat saturation in three orthogonal planes and one in abduction and external rotation position.^[34-36]

DISCUSSION

Planar approach

From prior studies, it can be concluded that tears can occur in any of the three planes (sagittal, coronal, and horizontal planes) of the SST.^[2-5] Most of the tears at footprint occur in the sagittal plane of tendon involving varying depths of

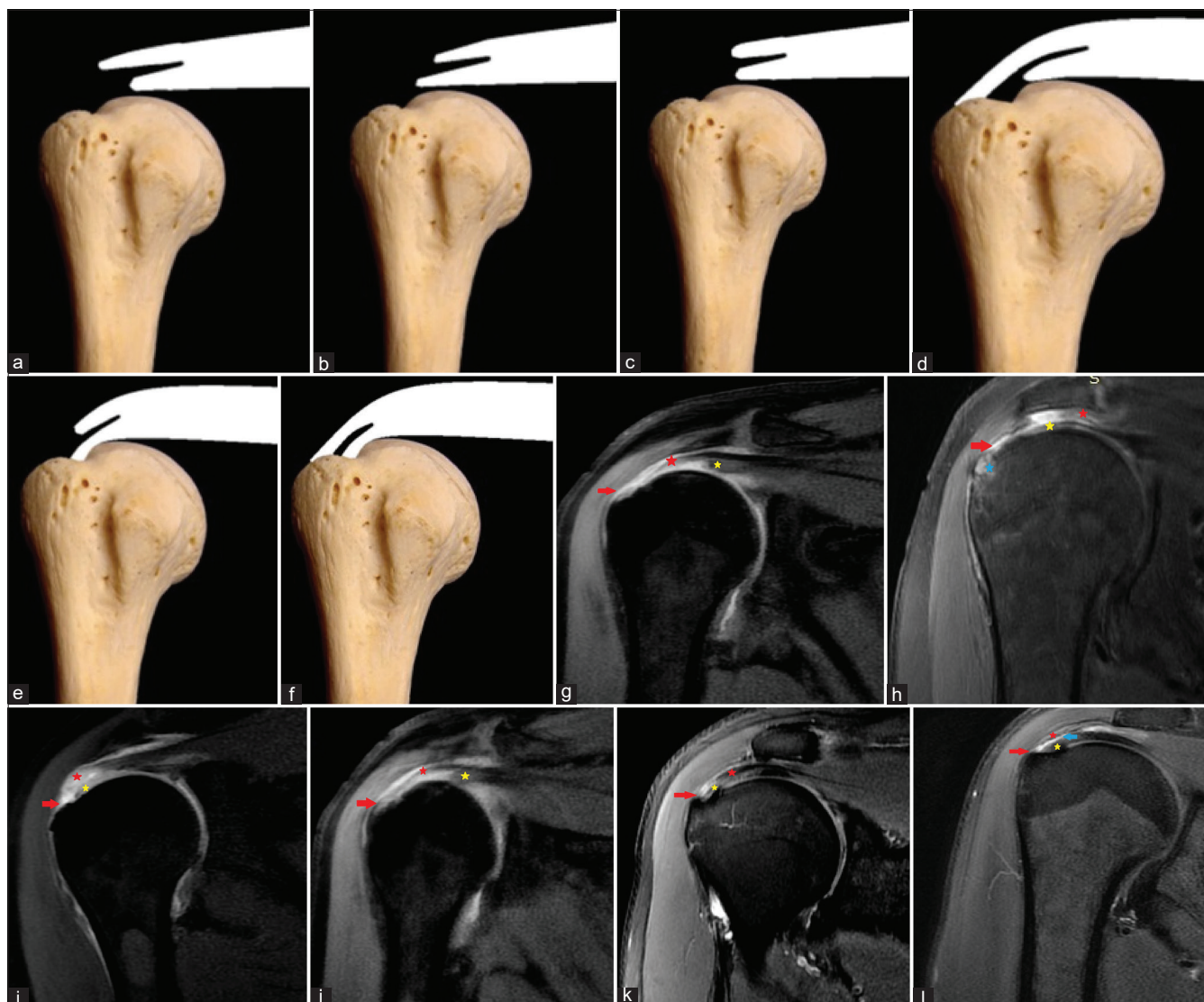


Figure 8: Schematic diagrams of the supraspinatus tendon (a-f) and representative oblique coronal proton-density fat saturation MR images (g-l) of the shoulder joint. The schematic diagrams demonstrate six types of delamination tears of the supraspinatus tendon. Representative MR images demonstrate tear at the footprint with extension into tendon substance in axial plane splitting articular and bursal fibers of the supraspinatus tendon (delamination tear). (a-c and g-i) Full-thickness tear at footprint with varying degrees of retraction of both articular and bursal fibers of the supraspinatus tendon. The retraction of articular fibers more than bursal fibers (a and g), Retraction of bursal fibers more than articular fibers (b and h), and equal degree of retraction of both articular and bursal fibers (c and i). (d, e and j, k) Partial-thickness tear at footprint with retraction of either articular (d and j) or bursal fibers (e and k) of the supraspinatus tendon. (f and l) Interstitial tear of the tendon without any extension to articular or bursal surface. (Red asterisk: Bursal fibers, yellow asterisk: Articular fibers, red arrow: Footprint, blue arrow: Interstitial tear, and blue asterisk: Subchondral cyst).

tendon thickness and are called partial thickness or full thickness. However, these footprint tears can extend further in the horizontal or longitudinal plane of the tendon. As the management depends on the type of supraspinatus footprint tears, the understanding of the planar orientation of SST tear at the footprint and its extension into tendon will help in management centric reporting by the practicing radiologists and radiology residents. Thus, a simplified 5-step algorithmic approach to describe SST tears at footprint is proposed:

Step 1 – Identification of a SST footprint tear: The presence of fluid signal within the SST footprint in the sagittal plane of the tendon is the hallmark of all SST footprint tears.

Step 2 – Determination of the thickness of the tear: Footprint tears can be classified as full-thickness or partial-thickness tears; the latter can be further graded using the Ellman classification and into the articular surface or bursal surface “[Figure 6].”^[2]

Step 3 – Identification of whether the tear is confined to the footprint: Such tears are called rim-vent tears. These appear on coronal oblique fluid sensitive sequences of MR images as a thin linear area of high signal adjacent to the horizontal superior portion of the greater tuberosity, interrupting the normal attachment of the articular surface cuff fibers.^[1] Their anteroposterior dimension determined on sagittal oblique images is typically greater than their mediolateral width measured on coronal oblique images “[Figure 9]”. Certain pitfalls must be avoided in the diagnosis of rim-vent tears. Intrasubstance high signal often seen in SSTs of older individuals, and the converging tendon of IST at the footprint should not be misinterpreted as rim-vent tears “[Figure 10].”

Step 4 – Identification of extension of footprint tear into the substance of tendon in the axial/horizontal plane of tendon: Such tears which extend into tendon substance in horizontal plane splitting between the articular and bursal layers of the SST are known as delamination tears. They are best appreciated on MRI in coronal oblique imaging.

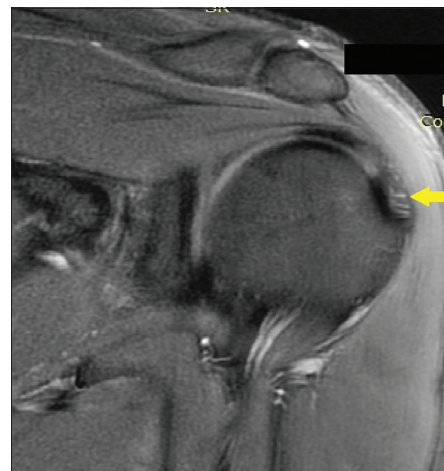


Figure 10: Oblique coronal proton-density fat saturation MR images of the shoulder joint demonstrate hyperintensities at footprint due to convergence of infraspinatus tendon fibers with posterior supraspinatus fibers (yellow arrow). Care is taken not to misinterpret it as rim-vent tear.



Figure 9: Schematic diagrams of the supraspinatus tendon (a and b) and representative oblique coronal (c) and oblique sagittal (d) proton-density fat saturation MR images of the shoulder joint. Schematic diagrams demonstrate a defect in the supraspinatus tendon at the footprint. Representative MR images demonstrate partial-thickness tear at the footprint of the supraspinatus tendon (yellow arrow), not extending into tendon substance. Note that the anteroposterior length of the tear is more than the mediolateral length.

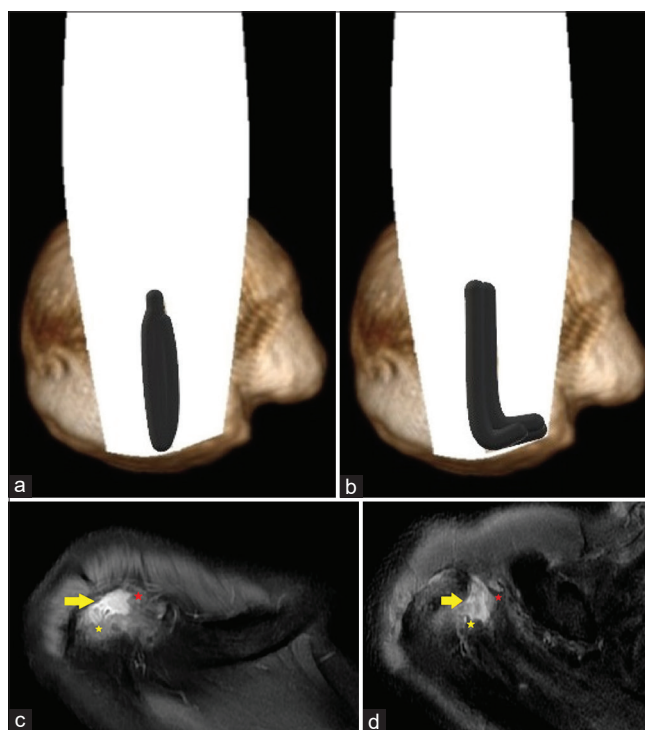


Figure 11: Schematic diagrams of the supraspinatus tendon (a and b) and representative axial proton-density fat saturation MR images (c and d) of the shoulder joint demonstrate footprint tear extending into tendon substance in coronal plane splitting into anterior and posterior fibers of the supraspinatus tendon (longitudinal tear). The geometry of longitudinal tear can be “U” shaped (a and c) or “L” shaped (b and d). (Yellow arrow: Footprint tear, red asterisk: Anterior fibers, and yellow asterisk: Posterior fibers).

These tears can have varying degrees of retraction of the articular surface and bursal surface fibers. The subtypes of delamination tear are determined based on the pattern of tear at the footprint in the sagittal plane (partial thickness/full thickness) and the pattern/degree of retraction of fibers.

According to Choo *et al.*,^[5] there is a full-thickness tear of supraspinatus at footprint (sagittal plane) in type 1a-c delamination tears, partial-thickness tear of supraspinatus



Figure 12: Oblique coronal proton-density fat saturation MR images of the shoulder joint demonstrate normal curvilinear smooth hyperintensity (blue arrow) at the interface of the long head of biceps tendon (red asterisk) and anterior-most fibers of the supraspinatus tendon (yellow asterisk). Care is taken not to misinterpret it as a longitudinal tear.

at footprint (sagittal plane) in type 2a, b, and interstitial tear at the footprint in Type 2c. Among the full thickness tears, type 1a has greater retraction of articular fibers than bursal fibers; type 1b has greater retraction of bursal fibers than articular fibers, while type 1c has equal retraction of articular and bursal fibers. Among partial-thickness tears, type 2a has retraction of articular fibers only, type 2b has retraction of bursal fibers only, while type 2c is an interstitial tear (no extension to articular/bursal surface, no retraction) “[Figure 8].”

Step 5 – Identification of extension of footprint tear into the substance of tendon in the coronal/longitudinal plane of tendon: Such tears that extend into the tendon substance in the coronal/longitudinal plane splitting between the anterior and posterior fibers of the SST are known as longitudinal tears. Similar to delamination tears, they can be subclassified based on the pattern of tear at the footprint in the sagittal plane as partial thickness or full thickness.

In contrast to rim-rent tears, longitudinal tears are relatively long and narrow. A U-shaped longitudinal tear has a smaller anteroposterior extent compared to the mediolateral extent; whereas an L-shaped longitudinal tear has nearly equal anteroposterior and mediolateral extents “[Figure 11].”^[4] Care must be taken not to misinterpret the interface of the long head of biceps tendon and anteriormost fibers of SST as longitudinal tear “[Figure 12].”

The plane-based approach for defining SST tear at footprint summarized in “[Figure 13].”

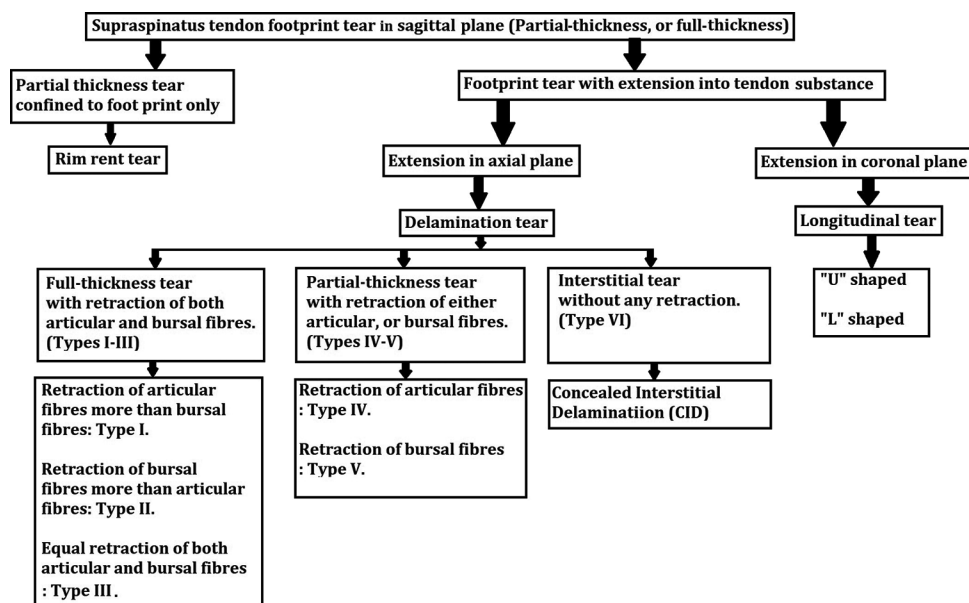


Figure 13: Flowchart demonstrating a step-by-step plane-based approach to characterize supraspinatus tendon tear at the footprint.

CONCLUSION

Partial- or full-thickness supraspinatus tears in the sagittal plane at footprint with or without extension into the substance of the tendon in the horizontal or longitudinal planes form the basis of our approach for describing these tears. This simplified planar approach will help the residents and musculoskeletal radiology practitioners to understand the architecture of the supraspinatus tear on MRI and clearly communicate the relevant findings to the arthroscopic surgeon. Simultaneously, it will also help the arthroscopic surgeons to more easily comprehend the type of tear and plan the appropriate repair procedure for a better surgical outcome. In the future, this model could also have applications in computer-aided detection and classification of footprint tears.

Learning points

- A planar-based approach to define the SST tear at the footprint and its extension into tendon on MRI will help in reporting by the practicing radiologists and radiology residents.
- Most of the SST tear at footprint occurs in the sagittal plane; partial thickness, fullthickness, or interstitial.
- Rim-vent tears are the footprint tear without any extension into the tendon.
- Delamination tears are the footprint tear that extends into the tendon in a horizontal plane splitting between the articular and bursal layers of the SST.
- Longitudinal tears are the footprint tears that extend into the tendon substance in the coronal plane splitting between the anterior and posterior fibers of the SST.

Declaration of patient consent

The patient consent is not required as the patient's identity is not disclosed or compromised.

Financial support and sponsorship

Nil.

Conflicts of interest

There are no conflicts of interest.

REFERENCES

1. Vinson EN, Helms CA, Higgins LD. Rim-vent tear of the rotator cuff: A common and easily overlooked partial tear. *AJR Am J Roentgenol* 2007;189:943-6.
2. Ellman H. Diagnosis and treatment of incomplete rotator cuff tears. *Clin Orthop Relat Res* 1990;254:64-74.
3. Schaeffeler C, Mueller D, Kirchoff C, Wolf P, Rummeny EJ, Woertler K. Tears at the rotator cuff footprint: Prevalence and imaging characteristics in 305 MR arthrograms of the shoulder. *Eur Radiol* 2011;21:1477-84.
4. Davidson J, Burkhart SS. The geometric classification of rotator cuff tears: A system linking tear pattern to treatment and prognosis. *Arthroscopy* 2010;26:417-24.
5. Choo HJ, Lee SJ, Kim JH, Kim DW, Park YM, Kim OH, *et al.* Delaminated tears of the rotator cuff: Prevalence, characteristics, and diagnostic accuracy using indirect MR arthrography. *AJR Am J Roentgenol* 2015;204:360-6.
6. Vosloo M, Keough N, De Beer MA. The clinical anatomy of the insertion of the rotator cuff tendons. *Eur J Orthop Surg Traumatol* 2017;27:359-66.
7. Curtis AS, Burbank KM, Tierney JJ, Scheller AD, Curran AR. The insertional footprint of the rotator cuff: An anatomic study. *Arthroscopy* 2006;22:609.e1.
8. Mochizuki T, Sugaya H, Uomizu M, Maeda K, Matsuki K, Sekiya I, *et al.* Humeral insertion of the supraspinatus and infraspinatus. New anatomical findings regarding the footprint of the rotator cuff. *J Bone Joint Surg Am* 2008;90:962-9.
9. Nakajima T, Rokuuma N, Hamada K, Tomatsu T, Fukuda H. Histologic and biomechanical characteristics of the supraspinatus tendon: Reference to rotator cuff tearing. *J Shoulder Elbow Surg* 1994;3:79-87.
10. Nimura A, Kato A, Yamaguchi K, Mochizuki T, Okawa A, Sugaya H, *et al.* The superior capsule of the shoulder joint complements the insertion of the rotator cuff. *J Shoulder Elbow Surg* 2012;21:867-72.
11. Clark JM, Harryman DT. Tendons, ligaments, and capsule of the rotator cuff: Gross and microscopic anatomy. *J Bone Joint Surg Am* 1992;74:713-25.
12. Spargoli G. Supraspinatus tendon pathomechanics: A current concepts review. *Int J Sports Phys Ther* 2018;13:1083-94.
13. Thomopoulos S, Genin GM, Galatz LM. The development and morphogenesis of the tendon-to-bone insertion-what development can teach us about healing. *J Musculoskelet Neuronal Interact* 2010;10:35-45.
14. van der Windt DA, Koes BW, de Jong BA, Bouter LM. Shoulder disorders in general practice: Incidence, patient characteristics, and management. *Ann Rheum Dis* 1995;54:959-64.
15. Vecchio P, Kavanagh R, Hazleman BL, King RH. Shoulder pain in a community-based rheumatology clinic. *Br J Rheumatol* 1995;34:440-2.
16. Milgrom C, Schaffler M, Gilbert S, van Holsbeeck M. Rotator-cuff changes in asymptomatic adults. The effect of age, hand dominance and gender. *J Bone Joint Surg Br* 1995;77:296-8.
17. Tempelhof S, Rupp S, Seil R. Age-related prevalence of rotator cuff tears in asymptomatic shoulders. *J Shoulder Elbow Surg* 1999;8:296-9.
18. Minagawa H, Yamamoto N, Abe H, Fukuda M, Seki N, Kikuchi K, *et al.* Prevalence of symptomatic and asymptomatic rotator cuff tears in the general population: From mass-screening in one village. *J Orthop* 2013;10:8-12.
19. Mall NA, Lee AS, Chahal J, Sherman SL, Romeo AA, Verma NN, *et al.* An evidenced-based examination of the epidemiology and outcomes of traumatic rotator cuff tears. *Arthroscopy* 2013;29:366-76.
20. Bey MJ, Song HK, Wehrli FW, Soslowsky LJ. Intratendinous strain fields of the intact supraspinatus tendon: The effect of

- glenohumeral joint position and tendon region. *J Orthop Res* 2002;20:869-74.
21. Nyffeler RW, Schenk N, Bissig P. Can a simple fall cause a rotator cuff tear? Literature review and biomechanical considerations. *Int Orthop* 2021;45:1573-82.
 22. Fukuda H. The management of partial-thickness tears of the rotator cuff. *J Bone Joint Surg Br* 2003;85:3-11.
 23. Bencardino JT, Garcia AI, Palmer WE. Magnetic resonance imaging of the shoulder: Rotator cuff. *Top Magn Reson Imaging* 2003;14:51-67.
 24. Stetson WB, Phillips T, Deutsch A. The use of magnetic resonance arthrography to detect partial-thickness rotator cuff tears. *J Bone Joint Surg Am* 2005;87:81-8.
 25. Codman EA. *The Shoulder; Rupture of the Supraspinatus Tendon and Other Lesions in or about the Subacromial Bursa*. New York: C. Miller; 1934.
 26. Snyder SJ, Pachelli AF, Del Pizzo W, Friedman MJ, Ferkel RD, Pattee G. Partial thickness rotator cuff tears: Results of arthroscopic treatment. *Arthroscopy* 1991;7:1-7.
 27. Burns JP, Snyder SJ. Arthroscopic rotator cuff repair in patients younger than fifty years of age. *J Shoulder Elbow Surg* 2008;17:90-6.
 28. Sonnabend DH, Yu Y, Howlett CR, Harper GD, Walsh WR. Laminated tears of the human rotator cuff: A histologic and immunochemical study. *J Shoulder Elbow Surg* 2001;10:109-15.
 29. Burkhart SS, Danaceau SM, Pearce CE Jr. Arthroscopic rotator cuff repair: Analysis of results by tear size and by repair technique-margin convergence versus direct tendon-to-bone repair. *Arthroscopy* 2001;17:905-12.
 30. Davidson JF, Burkhart SS, Richards DP, Campbell SE. Use of preoperative magnetic resonance imaging to predict rotator cuff tear pattern and method of repair. *Arthroscopy* 2005;21:1428.
 31. Burkhart SS. A stepwise approach to arthroscopic rotator cuff repair based on biomechanical principles. *Arthroscopy* 2000;16:82-90.
 32. Burkhart SS. Reconciling the paradox of rotator cuff repair versus debridement: A unified biomechanical rationale for the treatment of rotator cuff tears. *Arthroscopy* 1994;10:4-19.
 33. Helms CA, Major NM, Anderson MW, Kaplan PA, Dussault R. *Shoulder*. In: *Musculoskeletal MRI*. 2nd ed. Philadelphia, PA: Saunders; 2009. p. 177-223.
 34. Palmer WE, Caslowits PL, Chew FS. MR arthrography of the shoulder: Normal intraarticular structures and common abnormalities. *AJR* 1995;164:141-6.
 35. Flannigan B, Kursunoglu-Brahme S, Snyder S, Karzel R, Del Pizzo W, Resnick D. MR arthrography of the shoulder: Comparison with conventional MR imaging. *AJR Am J Roentgenol* 1990;155:829-32.
 36. Tirman PF, Bost FW, Steinbach LS, Mall JC, Peterfy CG, Sampson TG, *et al.* MR arthrographic depiction of tears of the rotator cuff: Benefit of abduction and external rotation of the arm. *Radiology* 1994;192:851-6.

How to cite this article: Sharma A, Gehlot K, Tomar S, Kumar M, Kumar N, Singh DK. A plane-based approach for the characterization of supraspinatus tendon tear at the footprint in MRI. *Indian J Musculoskeletal Radiol* 2022;4:3-12.